Contribution from the Department of Molecular Spectroscopy, Research Institute of Materials, University of Nijmegen, Toernooiveld, 6525 ED Nijmegen, The Netherlands

Electron Spin Echo Envelope Modulation Study of Bis(tetrabutylammonium) Bis(maleonitriledithiolato)nickelate(II) Doped with Copper(II)

E. J. Reijerse, A. H. Thiers, R. Kanters, M. C. M. Gribnau, and C. P. Keijzers*

Received December 5, 1986

The electron spin echo envelope modulation (ESEEM) technique is used to determine the ^{14}N hyperfine and quadrupole interaction tensors in bis(tetrabutylammonium) bis(maleonitriledithiolato)copper(II), 3% doped in the diamagnetic nickel(II) host. The line positions and peak intensities of the Fourier-transformed ESEEM spectra are interpreted by using simulated spectra. The latter are obtained by diagonalizing the full spin-Hamiltonian matrix, which includes interactions of the ^{63}Cu spin $I = {}^3/_2$ and two nonequivalent ^{14}N spins $I = 1$. Good agreement between the experimental and the simulated spectra is obtained. The ^{14}N hyperfine and quadrupole interactions are calculated with molecular orbital coefficients obtained with an extended Hückel method. In the calculation of the hyperfine interactions, two- and three-center contributions are included. The correspondence with the experimental tensors is astonishing! In the interpretation of the electronic structure a comparison is made with earlier work on copper(II)/nickel(II) bis(*N*,*N*'-di-*n*-butyldithiocarbamate).

Introduction

Complexes of transition metals with dithiolene ligands have been studied extensively with EPR and various other techniques[1-9] because of their interesting properties: formation of 1-dimensional conductors[3,10] and π-donor-acceptor complexes[11-13] and the stabilization of rare, formal oxidation states.[14,15] In particular the rare oxidation states, but probably also the other properties, are caused by the highly covalent character of the metal-sulfur bond, which causes the actual charge of the metal ion to be much smaller than the formal charge. This highly covalent character is confirmed by molecular orbital (MO) calculations[8] and, as far as the unpaired spin density is concerned, by EPR experiments.[1] With EPR, and especially with related methods such as ENDOR, it has recently been possible to measure hyperfine interactions (HFI's) with the sulfur atoms[16] and also with the atoms in the second and higher coordination spheres.[8,9] This has resulted in a very good insight into the electronic structure of these systems, especially the density distribution of the unpaired electron. Therefore, these molecules are very good test systems for MO calculations and also for new experimental techniques.

Electron spin-echo envelope modulation (ESEEM) is a technique that although it was described many years ago,[17,18] has been reaching perfection only in the past few years. The advantage of this technique, as compared to ENDOR, is that the line intensities are not influenced by relaxation effects so that they can be calculated more easily, *in principle*. A disadvantage of this technique is that the spectra may be very complicated, especially for quadrupolar nuclei and certainly for powder samples. In order to analyze these spectra, it is necessary to be able to generate reliable simulations. This is the reason that a number of papers have recently been published, with theoretically calculated spectra with which the limits of the interpretations have been tested.[19-21]

In order to judge the quality of the calculated spectra one needs to compare them with good quality experimental spectra. For that purpose powder samples are difficult, especially if the *g* value is isotropic, because in that case all orientations are simultaneously excited. Single crystals are, therefore, much better suited to this purpose. This is why we recently measured the ^{14}N interactions in the system copper bis(*N*,*N*'-di-*n*-butyldithiocarbamate) (Cu(dtc)$_2$) doped in the diamagnetic nickel host.[22] Although Cu(dtc)$_2$ is a simple system with only two equivalent (inversion symmetry) nitrogen atoms, the analysis of the spectra was quite difficult since the HFI, the nuclear quadrupole interaction (NQI), and the nuclear Zeeman interaction (NZI) were all of the same order of magnitude. In a second paper we published the powder spectra of this system and also the simulated spectra, which were in excellent agreement with the experimental spectra.[23]

The system copper bis(maleonitriledithiolate)(2-) (Cu(mnt)$_2^{2-}$) diluted in the diamagnetic nickel(II) host is a challenge because this molecule contains two sets of two equivalent nitrogen atoms (see I) so that the spectra are expected to be much more complex.

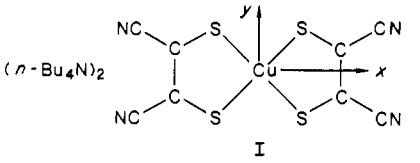

I

An additional complication in the Cu(mnt)$_2^{2-}$ system is that the distance from the Cu to the N (in the fourth coordination sphere) is 5.6 Å. This is larger than the 4.0 Å separation between Cu and N (in the third coordination sphere) in Cu(dtc)$_2$. Thus a different ratio of the HFI, NQI, and NZI is expected, which makes this system another, demanding, test for our ESEEM simulation

(1) Maki, A. H.; Edelstein, N.; Davidson, A.; Holm, R. H. *J. Am. Chem. Soc.* **1964**, *86*, 4580.
(2) Plumlee, K. W.; Hoffman, B. M.; Ratjack, M. T.; Kannenwurf, C. R. *Solid State Commun.* **1974**, *15*, 1651.
(3) Plumlee, K. W.; Hoffman, B. M.; Ibers, J. A.; Soos, Z. G. *J. Chem. Phys.* **1975**, *63*, 1926.
(4) White, L. K.; Belford, R. L. *J. Am. Chem. Soc.* **1976**, *98*, 4428.
(5) Kirmse, R.; Stach, J.; Dietzsch, W.; Hoyer, E. *Inorg. Chim. Acta* **1978**, *26*, L53.
(6) Inone, M.; Hiroyoshi, K.; Nakamusa, D. J. *J. Magn. Reson.* **1979**, *33*, 409.
(7) Snaathorst, D.; Doesburg, H. M.; Perenboom, J. A. A. J.; Keijzers, C. P. *Inorg. Chem.* **1981**, *20*, 2526.
(8) Kirmse, R.; Stach, J.; Abram, U.; Dietzsch, W.; Böttcher, R.; Gribnau, M. C. M.; Keijzers, C. P. *Inorg. Chem.* **1984**, *23*, 3333.
(9) Stach, J.; Kirmse, R.; Sieler, J.; Abram, U.; Dietzsch, W.; Böttcher, R.; Hansen, L. K.; Vergoossen, H.; Gribnau, M. C. M.; Keijzers, C. P. *Inorg. Chem.* **1986**, *25*, 1369.
(10) Interrante, L. V.; Browall, K. W.; Hart, H. R., Jr.; Jacobs, I. S.; Watkins, G. D.; Wee, S. H. *J. Am. Chem. Soc.* **1975**, *97*, 889.
(11) Schmitt, R. D.; Wing, R. M.; Maki, A. H. *J. Am. Chem. Soc.* **1979**, *91*, 4394.
(12) Wing, R. M.; Schlupp, R. L. *Inorg. Chem.* **1970**, *9*, 471.
(13) Manoharan, P. T.; Noordik, J. H.; de Boer, E.; Keijzers, C. P. *J. Chem. Phys.* **1981**, *74*, 1980.
(14) van Rens, J. G. M.; Viegers, M. P. A.; de Boer, E. *Chem. Phys. Lett.* **1974**, *28*, 104.
(15) Schlupp, R. L.; Maki, A. H. *Inorg. Chem.* **1974**, *13*, 44.
(16) Kirmse, R.; Dietzsch, W.; Stach, J.; Golic, L.; Böttcher, R.; Brunner, W.; Gribnau, M. C. M.; Keijzers, C. P. *Mol. Phys.* **1986**, *57*, 1139.
(17) Mims, W. B. *Phys. Rev. B: Solid State* **1972**, *5*, 2409.
(18) Mims, W. B. *Phys. Rev. B: Solid State* **1972**, *6*, 3543.
(19) Astashkin, A. V.; Dikanov, S. A.; Tsvetkov, Yu, D. *Chem. Phys. Lett.* **1985**, *122*, 259.
(20) de Groot, A.; Evenlo, R.; Hoff, A. J. *J. Magn. Reson.* **1986**, *66*, 331.
(21) Reijerse, E. J.; Keijzers, C. P. *J. Magn. Reson.* **1987**, *71*, 83.
(22) Reijerse, E. J.; Paulissen, M. L. H.; Keijzers, C. P. *J. Magn. Reson.* **1984**, *60*, 66.
(23) Reijerse, E. J.; van Aerle, N. A. J. M.; Keijzers, C. P.; Böttcher, R.; Kirmse, R.; Stach, J. *J. Magn. Reson.* **1986**, *67*, 114.

0020-1669/87/1326-2764$01.50/0

Table I. Experimental and Calculated Tensors in the Axis System of A^{Cu} [a] and in the Molecular Axis System, Respectively, at a Temperature of 30 K (HFI and NQI in MHz)

		exptl				calcd			
			axis[a]				axis		
		values	A_1	A_2	A_3	values	x	y	z
	g_1	2.018	35	55	91	2.021	1	90	91
	g_2	2.022	55	145	86	2.024	90	0	90
	g_3	2.086	92	86	5	2.079	89	90	1
^{63}Cu	A_1	120.6	0	90	90	118.1	14	76	89
	A_2	134.1	90	0	90	117.3	102	14	90
	A_3	−254.7	90	90	0	−235.3	90	90	1
	A_{iso}	−256.5				−35.7			
$^{14}N_1$	A_1	−0.318	34	111	65	−0.315	24	114	86
	A_2	−0.486	112	80	25	−0.483	89	80	11
	A_3	0.804	66	24	90	0.798	66	26	100
	A_{iso}	0.306				0.177			
$^{14}N_2$	A_1	−0.249	41	63	62	−0.273	21	70	87
	A_2	−0.471	116	100	27	−0.435	90	89	9
	A_3	0.720	61	151	86	0.708	69	157	108
	A_{iso}	0.231				0.174			
$^{14}N_1$	P_1	0.779	87	91	3	0.540	96	91	6
	P_2	1.046	62	28	91	0.806	58	32	86
	P_3	−1.826	28	118	93	−1.346	32	122	86
$^{14}N_2$	P_1	0.821	82	96	10	0.546	95	87	6
	P_2	1.103	57	145	110	0.800	60	149	85
	P_3	−1.925	34	56	93	−1.346	31	60	87

[a] The directions of the principal axes A_1, A_2, and A_3 of the ^{63}Cu HFI tensor relative to the molecular axes x, y, and z were not determined because the crystal was not oriented with X-ray diffraction. However, Maki et al.[1] found that $A_1 \| x$, $A_2 \| y$, and $A_3 \| z$.

program, which recently has been considerably improved.

Another reason to study this system with ESEEM is that although CW-ENDOR was successfully used to measure the ^{13}C HFI[8] (also in the nonplanar Zn host[9]) of the ring- and CN-carbon atoms, ^{14}N interactions could only be observed in a few directions. This was rather surprising because $Cu(dtc)_2$ caused no problem at all for the CW technique, either for the ^{13}C[24,25] or for the ^{14}N[25,26] interactions. A possible explanation is that the NMR transition probabilities are larger in $Cu(dtc)_2$ because of a larger HFI (smaller Cu–N distance). In this paper we compare and discuss the calculated dtc and mnt spectra. The techniques are reported in the Experimental Section, and the experimental results are presented in the subsequent section. In the last part of this paper the experimental results are discussed on the basis of MO calculations and elaborate computations of the spin-Hamiltonian parameters.

Experimental Section

The measurements were performed at 30 K in an Oxford Instruments CF200 helium flow cryostat. With two orthogonal rotation axes (one obtained by rotating the magnet, the second one being a goniometer in the cryostat) every crystal orientation relative to the magnetic field can be reached. With the help of field-swept spectra, the crystal was oriented in the principal axis system of the **g** tensor. These spectra were measured by monitoring the intensity of a two-pulse echo (pulse sequence $\pi/2 - \tau - \pi - \tau -$ echo, $\tau = 210$ ns) while the dc magnetic field was swept.

Spectra were measured at orientation intervals of 5–10°. From the field-swept spectra, the **g** tensor and the copper HFI tensor were obtained, which could then be compared with literature data[1,27] in order to judge the accuracy of the measurements.

The ESEEM spectra were measured with the stimulated echo sequence ($\pi/2 - \tau - \pi/2 - T - \pi/2 - \tau -$ echo, $\tau = 210$ ns, repetition time = 3 ms) by sweeping the time T from 0.80 to 26.35 μs in steps of 50 ns. The length of the $\pi/2$ pulses was 20 ns. In order to improve the signal-to-noise ratio, 50 echoes were averaged in a boxcar integrator (PAR 162/164) for every value of T. The echo signal-to-noise ratio was high enough to limit the experiment to 20 scans of T. The data were collected and processed in a MINC 11/23 minicomputer with home-written software. The modulation envelopes were transformed into the frequency domain by using standard procedures: high-pass filtering (cutoff frequency 50 kHz) and Fourier transformation. Dead time is not a serious problem in these *single-crystal* spectra (dead time after the third microwave pulse was 210 ns whereas the T sweep ranged from 0.8 to 26.35 μs). The phase errors that are the result of the dead time were not corrected; instead, the frequency domain spectra were transformed to the amplitude mode. The spectrometer has been described previously.[22] The magnetic field and the microwave frequency were measured with a Bruker B-NM12 gaussmeter and a Hewlett-Packard 5246L counter, respectively.

The copper and nickel complexes, $(NBu_4)_2M(mnt)_2$; M = Cu, Ni), were synthesized according to the literature method.[28] Single crystals with ~1% Cu in the diamagnetic Ni(II) crystal were grown by slow solvent evaporation of an acetone/ethanol solution of the two complexes in a 1% concentration ratio.

Experimental Results

Both guest and host crystallize in the triclinic space group $P\bar{1}$ with $Z = 1$. In the host crystal, the mnt anions are separated by the bulky $N(n\text{-but})_4^+$ counterions,[29] whereas in the pure copper crystal the anions form linear stacks.[3] If the guest molecules accept the host structure, as was concluded from ^{13}C ENDOR measurements,[8] the anion is nearly planar and close to D_{2h} symmetry.

In accord with the crystal structure the echo-induced (field-swept) spectra show the resonance of only one molecule, which is split by the interaction with the copper nuclear spin. The measured principal values of the **g** tensor and the ^{63}Cu HFI tensor are listed in Table I. They are close to the room-temperature values, which were measured with CW EPR.[1] The crystal was oriented in the axis system of the copper HFI tensor by using the field-swept spectra. We have assumed that the copper HFI axis system coincides with the molecular axis system ($A_1 // x$, $A_2 // y$, and $A_3 // z$; see I), following the findings of Maki et al.[1] Because of the near axiality of the **g** tensor, the experimental error in the position of its in-plane axes is rather large and the angle of 35° between A_1 and g_1 has a large error.

Figure 1A shows the experimental ESEEM spectra in the three measured planes after Fourier transformation and transformation to amplitude mode. Every spectrum has peaks in the region below

(24) Kirmse, R., Abram, U.; Böttcher, R. *Chem. Phys. Lett.* **1982**, *88*, 98.
(25) Kirmse, R., Abram, U.; Böttcher, R. *Chem. Phys. Lett.* **1982**, *90*, 9.
(26) Böttcher, R.; Kirmse, R.; Stach, J.; Reijerse, E. J.; Keijzers, C. P. *Chem. Phys.* **1986**, *107*, 145.
(27) White, L. K.; Belford, R. L. *J. Am. Chem. Soc.* **1976**, *98*, 4428.
(28) Davidson, A.; Holm, R. H. *Inorg. Synth.* **1971**, *10*, 8.
(29) Kobayashi, A.; Sasaki, Y. *Bull. Chem. Soc. Jpn.* **1977**, *50*, 2650.

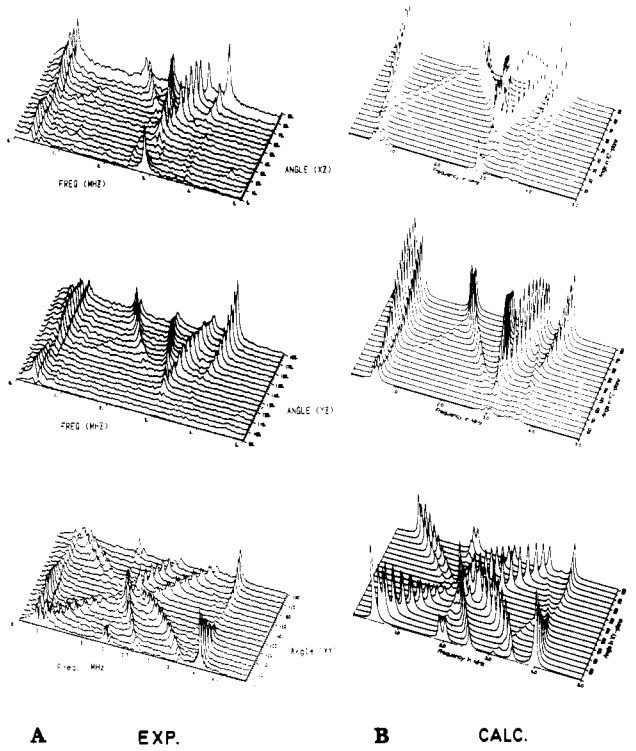

Figure 1. (A) Experimental FT-ESEEM spectra (amplitude mode) of $Cu/Ni(mnt)_2$ measured in three planes. Experimental data: three-pulse echo; pulse length = 20 ns; τ = 210 ns; T is stepped from 0.80 to 26.35 μs in steps of 50 ns. (B) Simulated FT-ESEEM spectra according to Hamiltonian (1) with τ = 210 ns.

1 MHz. These peaks do not fit the transitions of the cyanide nitrogen atoms, especially in the *xy* plane. Therefore, they are thought to arise from the dipolar interaction between the unpaired electron and the nitrogen atoms of the $N(n\text{-but})_4^+$ counterions. This Cu–N distance is 4.686 Å (in the host structure), almost 1 Å smaller than the distance between copper and the cyanide nitrogens.

Another rather puzzling feature of the experimental spectra is the splitting that is observed on several peaks in the *xy* and *yz* plane. The splittings vary between 40 and 80 kHz with a maximum value at orientations of maximum angular dependence of the peak positions. The nature of these splittings is not understood as will be discussed in the next section. In the fitting procedure of the tensors, the average frequency positions were used.

The frequencies of the peaks that are assigned to the cyanide nitrogens are plotted in Figure 2. Assigning these frequencies to the correct M_s manifold of the correct nitrogen atom is not straightforward. However, since all peaks (six for each nitrogen atom because I = 1) were observed, it was possible to select the three frequencies belonging to one M_s manifold by demanding that the sum of two of the frequencies equals the third (see Figure 3). These three transitions were used to determine the nitrogen HFI and NQI tensors in the following way: the transition frequencies were calculated with the spin Hamiltonian

$$H = \mu_B \mathbf{B}\cdot\mathbf{g}\cdot\mathbf{S} + \mathbf{S}\cdot\mathbf{A}^{Cu}\cdot\mathbf{I}^{Cu} - g_{Cu}\mu_n\mathbf{B}\cdot\mathbf{I}^{Cu} + \mathbf{I}^N\cdot\mathbf{P}^N\cdot\mathbf{I}^N + \mathbf{S}\cdot\mathbf{A}^N\cdot\mathbf{I}^N - g_N\mu_n\mathbf{B}\cdot\mathbf{I}^N \quad (1)$$

and subsequently the error function

$$\sum_i (\nu^i_{obsd} - \nu^i_{calcd})^2 \quad (2)$$

was minimized by varying the elements of $\mathbf{P}^N$ and $\mathbf{A}^N$. In (2) the summation runs over the three assigned transitions at all orientations of the magnetic field in the three measured planes. After minimization, the frequencies of the transitions in the other M_s manifold could be calculated and compared with the experimental data. In this way, the frequencies of the two nitrogen atoms could be separated. In a second run the transition frequencies of both M_s manifolds were included in the fitting procedure. The resulting principal values and the axes of the nitrogen tensors are listed in Table I. The largest quadrupole interaction (in absolute value) is in the direction of the C–N bond (deviation of ~3°) for both

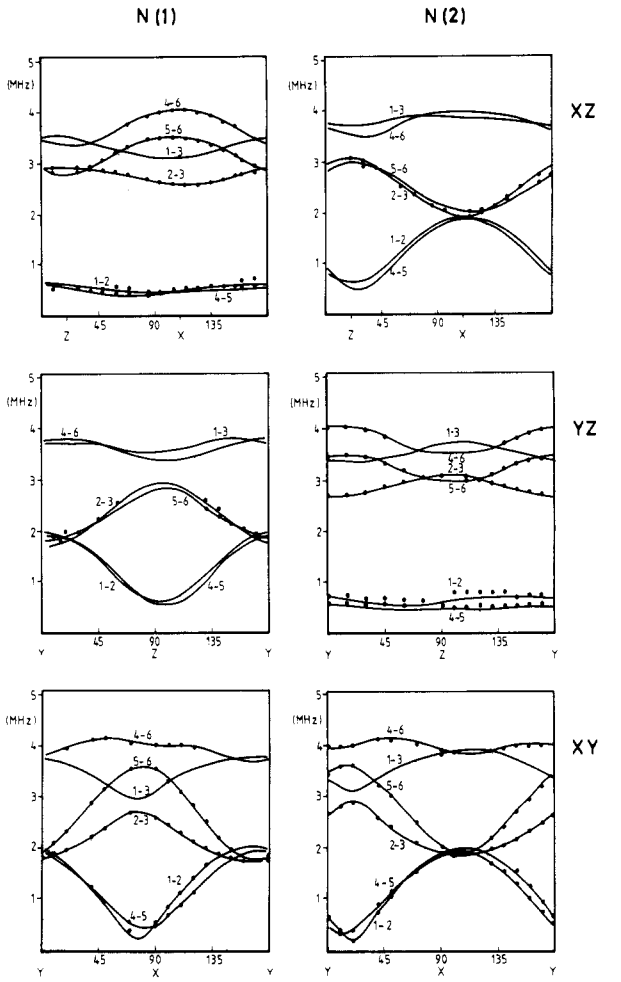

Figure 2. Frequencies of ^{14}N-ESEEM modulations assigned to CN groups. The numbering refers to the six-level energy diagram of one electron spin coupled to a ^{14}N nuclear spin in Figure 3. The fitted curves are indicated by the solid lines.

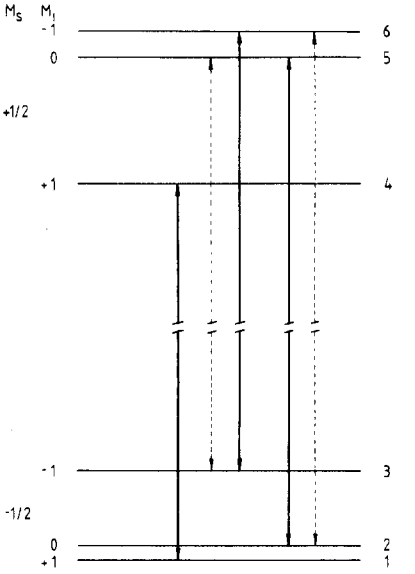

Figure 3. Energy level diagram for $S = {}^1/_2$ and ^{14}N nuclear spin I = 1 with B_0 at an arbitrary orientation. The forbidden transitions are indicated with dotted lines.

nitrogen atoms, and the smallest principal value is perpendicular to the molecular plane. Both atoms have the same value for the asymmetry parameter η ($=|(P_1 - P_2)/P_3|$), which is ~0.15, but the magnitude of the tensor elements differs by ~7%. The magnitude of the HFI is about 50% of the NQI. The isotropic contribution is one-third of the largest anisotropic principal value. The latter differs by about 10% for the two atoms and is located in the molecular plane, almost perpendicular to the C–N bond (~95°). The other two principal axes have no special orientations.

Simulation of Experimental Spectra

The FT-ESEEM spectra were simulated with the program MAGRES (MAGnetic RESonance) with the equations derived by Mims[17,18] for the stimulated echo sequence, in a generalized way:

$$P_{kn} = N\{\chi_{kn} + \sum_{i>j} 2\chi_{ij,kn} \cos(\omega_{ij}\tau)\} \quad (3)$$

where

$$\chi_{kn} = \sum_i |M_{ik}|^2 |M_{in}|^2$$

$$\chi_{ij,kn} = \mathrm{Re}\,[M^*_{ik} M_{in} M^*_{jn} M_{jk}]$$

P_{kn} is the modulation intensity of NMR transition k–n and M_{ik} is the transition moment between states i and k of the spin system. The indices i, j, k, and n run over all energy levels of the spin system. Inclusion of all four nitrogens in the spin-Hamiltonian (1) would give rise to a dimensionality of 648, which is too large to be handled by the simulation program (it would take 6.7 Mbyte to store the H matrix). Therefore, only two inequivalent ^{14}N nuclei were included. For τ the experimental value of 210 ns was used. The program MAGRES allows the calculation of EPR, ENDOR (without relaxation), ESEEM, and high-resolution NMR spectra for single crystals and powders with (in principle) any spin-Hamiltonian. Frequencies of peaks can be used to derive the tensor elements via a minimization procedure. ESEEM spectra are calculated in the frequency domain. Via a Fourier transformation the time domain can be computed. Dead-time effects can be simulated by a deletion of the dead-time part of the time domain, followed by a back-transformation to the frequency domain. Since in the present system dead time was not a serious problem, only the uncorrected frequency domain spectra were calculated. Hence, the influence of the dead time and the transformation to the amplitude mode were not simulated.

The simulated spectra are presented in Figure 1B. A comparison with the corresponding (Fourier-transformed) experimental spectra shows an excellent agreement in peak intensities and positions except for the small splittings in transition 5–6 in the yz plane and the larger splittings in transitions 1–2, 4–5, and 5–6 in the xy plane. ESE-ENDOR studies on $Cu/Ni(mnt)_2$ oriented near the x axis (an orientation where the ESEEM splittings were not resolved) also showed splittings of 5 kHz![30] Similar splittings were observed in ESEEM spectra of copper bis(*N*,*N*′-di-*n*-butyldithiocarbamate), $Cu(Bu_2dtc)_2$,[22] and an angular dependent line broadening was observed in CW-ENDOR spectra of copper bis(dialkyldithiocarbamate), $Cu(R_2dtc)_2$, and bis(dialkyldiselenocarbamate) doped in the Zn and Ni hosts.[26] Also in these two systems, the splitting/broadening was observed in those orientations where the lines have their maximum angular dependence. In order to investigate the possibility that these splittings are caused by second-order interactions between the four nitrogen spins, simulated spectra were calculated without the copper spin but including all four nitrogen spins and their interactions according to Hamiltonian (1). (As stated above, including the copper spin causes the dimensionality of the problem to become too large.) However, no evidence was found for splittings. Another possible cause would be a direct dipolar interaction between the cyanide N and a counterion proton. Evaluation of this interaction at a distance of 2.5 Å yields a maximum value of 1 kHz, which is much too small to account for the observed splittings. Optical and EPR studies of $Cu/Ni(mnt)_2$ by Manoharan et al.[31] suggested a change of crystal symmetry below 50 K that gave rise to splittings in the EPR spectrum. In our studies no splitting in the EPR spectra could be observed. However, such a drastic effect would hardly explain the very small splittings in our ESEEM spectra. Moreover, the ESEEM splittings are temperature independent up to 70 K. Nevertheless, these findings suggest the possibility of a breakdown of molecular inversion symmetry, which would give rise to four inequivalent nitrogens. It is not clear, however, why similar effects were not observed in earlier ^1H and ^{13}C CW-ENDOR studies of the same compounds.

As was mentioned in the introduction, no good ^{14}N CW-ENDOR spectra of this system could be obtained[8] in contrast to the system $Cu(dtc)_2$ where strong lines were observed.[25,26] In order to check whether this difference is due to the different magnitudes of the NQI and HFI, the nuclear spin transition probabilities of both complexes were calculated with the experimentally determined spin-Hamiltonian parameters. Indeed, the NMR transition moments of mnt were significantly lower than those of dtc (about a factor of 3). Moreover, the number of "strong" NMR transitions, i.e. with transition moments larger than 0.1×10^{-8}, was systematically lower in mnt (average of three) than in dtc (average of five). It is not clear, however, that this is the only reason for the weak ^{14}N CW-ENDOR spectra of mnt, since dtc ENDOR transitions that were calculated to be "weak" could still be detected in many cases.

Discussion

The **g** tensor and the copper HFI tensor agree with previous literature data.[1,8] The nitrogen HFI and NQI tensors were not determined previously because the CW-ENDOR signals were too weak for a full rotational study.[8] The nitrogen interactions were measured with ESEEM or CW-ENDOR in a series of $Cu(R_2dtc)_2$ (II) molecules in two different host crystals.[26]

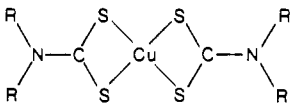

II

A comparison between the nitrogen tensors in dtc and mnt shows large differences:

1. In the present system the largest hyperfine and quadrupole components are located in the molecular plane (parallel and perpendicular to the C–N bond respectively), whereas in the dithiocarbamate molecules they are perpendicular to the molecular plane.
2. In the $Cu(mnt)_2^{2-}$ molecule, the tensors are less axial, with an asymmetry parameter of 0.15 for the NQI and asymmetry parameters of 0.21 and 0.31 for the HFI.
3. The NQI is ~30% larger than that in the dtc system.
4. The isotropic HFI is a factor of 3 smaller whereas the anisotropic part of the HFI tensor is almost a factor of 2 larger than those in $Cu(R_2dtc)_2$. This is very remarkable because the copper–nitrogen distance is much larger in the $Cu(mnt)_2^{2-}$ molecule, where the nitrogen is located in the fourth coordination sphere whereas the nitrogen is in the third coordination sphere in $Cu(R_2dtc)_2$.

These differences suggest that the spin-density and electron-density distributions in the C–N and the C–N(–C)$_2$ fragments in $Cu(mnt)_2^{2-}$ and $Cu(dtc)_2$ respectively, are very different. Several papers[7-9,22,32,33] have been published with molecular orbital (MO) calculations on these molecules, the results of which were, in turn, used for the computation of the spin-Hamiltonian parameters. The calculations resulted in good fits of the **g** tensor and the copper and sulfur HFI tensors for both molecules. For $Cu(dtc)_2$, ^1H, ^{13}C, and ^{14}N HFI tensors were also calculated and compared with those from ENDOR and ESEEM experiments.[22,32,33] For $Cu(mnt)_2^{2-}$ the ^{13}C HFI tensors were calculated

(30) Reijerse, E. J.; Klaassen, A. A. K. *Rev. Sci. Instrum.* **1986**, *57*, 2768.
(31) Manoharan, P. T.; Chandramouli, G. V. R., personal communication.
(32) Keijzers, C. P.; Snaathorst, D. *Chem. Phys. Lett.* **1980**, *69*, 348.
(33) Snaathorst, D.; Keijzers, C. P.; Klaassen, A. A. K.; de Boer, E.; Chacko, V. P.; Gomperts, R. *Mol. Phys.* **1980**, *40*, 585.

Table II. LCAO Coefficients of Nitrogen Orbitals in the Molecular Orbital of the Unpaired Electron

		$Cu(Et_2dtc)_2$	$Cu(mnt)_2^{2-}$
N(1)	3s	−0.0001	0.0091
	$3p_x$	−0.0012	−0.0436
	$3p_y$	−0.0089	−0.0898
	$3p_z$	0.0016	0.0173
N(2)	3s		−0.0090
	$3p_x$		0.0370
	$3p_y$		−0.0871
	$3p_z$		−0.0144

in order to compare them with ENDOR data. The ^{14}N HFI or NQI were not calculated for this system. Therefore, in this paper we concentrate on the calculation of these interactions in order to compare them with the experimental tensors and to compare the electronic structure around the nitrogen nuclei in $Cu(R_2dtc)_2$ and $Cu(mnt)_2^{2-}$. In the MO calculations, an extended Hückel method was used with the same empirical parameters as were used previously.[8,32] The structure of the $Cu(mnt)_2^{2-}$ molecule was assumed to be the same as that of the nickel molecule in the host crystal with two alterations:

1. The ligands were shifted by 0.06 Å along the x axis, which results in a copper–sulfur distance that is in between the metal–sulfur distances of the guest and the host molecules.

2. The computation of the nitrogen interactions turned out to be very sensitive to the C–N bond length and bond direction. In the host crystal the C–N bond lengths are different (1.130 and 1.147 Å) and both bonds point to one side of the molecular plane.[29] In the pure copper crystal, the C–N bond lengths are equal (1.144 and 1.143 Å), and one bond points above the plane, the other below the plane.[3] Therefore, the C–N distances in the copper crystal and the C–N directions of the host crystal were used.

The picture that emerges from the calculations is that about 50% of the unpaired electron is centered on the d_{xy} orbital of the copper atom. The remaining 50% is delocalized on the four sulfur atoms. The spin density on the remaining ligand atoms is very small. In Table II we have listed the coefficients of the nitrogen orbitals together with coefficients of the $Cu(et_2dtc)_2$ molecule.[32] At first sight it seems surprising that the spin density on the nitrogen in the present system is larger, even though the nitrogen atom is at a larger distance from the copper atom. However, in $Cu(R_2dtc)_2$ the nitrogen atom is located in a nodal plane of the B_{1g} MO (in the approximation of D_{2h} symmetry) and only the $2p_y$ orbital can have a spin density. However, the overlap of the nitrogen orbitals with the sulfur orbitals is small, and hence, the mixing is small. In $Cu(mnt)_2^{2-}$, the $2p_x$ and $2p_y$ orbitals of the nitrogens can mix into the unpaired electron MO (also B_{1g} in D_{2h} symmetry) and the overlap with the sulfur orbitals is, therefore, much more favorable.

The **g** tensor, HFI, and NQI tensors were calculated according to formulas that were published earlier.[34] They are listed in Table I. The **g** tensor and the copper HFI tensor agree very well with the experimental results, demonstrating that the calculated MO energies and coefficients are reliable. In the calculation of the copper HFI, only one-center integrals[32] were included in both first- and second-order contributions. This approximation is not valid for the nitrogen HFI because the multicenter integrals are expected to yield a sizable contribution due to the fact that almost all of the spin density is located on copper and sulfur. The calculated second-order contribution is small, and hence, multicenter integrals are calculated only in the first-order contribution. This first-order contribution is brought about by the electron-spin–nuclear-spin dipole–dipole interaction (e.g. with nucleus N) and can be expressed as[32]

$$A^N_{ij} = \left(\frac{\mu_0}{4\pi}\right) g_e g_N \mu_B \mu_n \left\langle \psi_0 \left| \frac{F^N_{ij}}{r_N^3} \right| \psi_0 \right\rangle \qquad (4)$$

(34) Keijzers, C. P.; de Boer, E. *Mol. Phys.* **1975**, *29*, 1007.
(35) Geurts, P. J. M.; Bouten, P. C. P.; van der Avoird, A. *J. Chem. Phys.* **1980**, *73*, 1306.

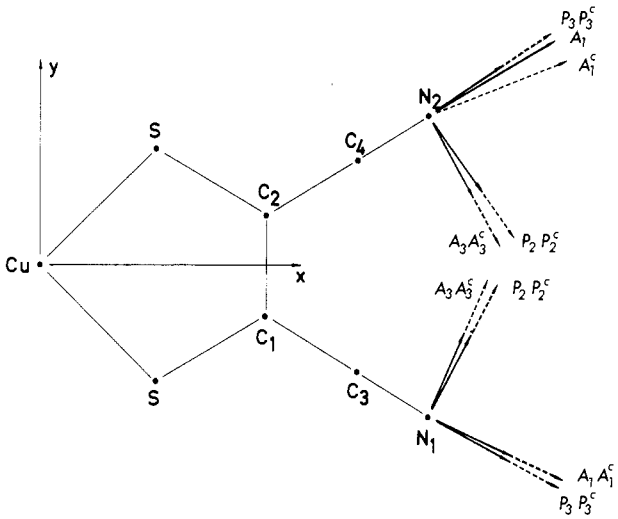

Figure 4. Orientation of the experimental (**A**, **P**) and the calculated ($\mathbf{A}^c$, $\mathbf{P}^c$) ^{14}N tensors.

where μ_0 is the permeability of free space, μ_B is the Bohr magneton, μ_n is the nuclear magneton, g_e is the free-electron g value, and g_N is the gyromagnetic ratio of nucleus N; i, j are x, y, z, F^N_{ij} is a component of a symmetric traceless tensor operator related to the dipolar interaction and r_N is the electron–nucleus radius vector. If ψ_0, the MO of the unpaired electron, is expanded as a linear combination of atomic orbitals, ϕ^A_i, centered on nuclei A, then eq 4 can be rewritten:

$$A^N_{ij} = \left(\frac{\mu_0}{4\pi}\right) g_e g_N \mu_B \mu_n \left\{ \sum_{i\in N}\sum_{j\in N} \left\langle C^N_i \phi^N_i \left| \frac{F^N_{ij}}{r_N^3} \right| C^N_j \phi^N_j \right\rangle + \sum_{A\neq N}\sum_{i\in A}\sum_{j\in A} \left\langle C^A_i \phi^A_i \left| \frac{F^N_{ij}}{r_N^3} \right| C^A_j \phi^A_j \right\rangle + \sum_{A\neq N}\sum_{i\in A}\sum_{j\in N} \left\langle C^A_i \phi^A_i \left| \frac{F^N_{ij}}{r_N^3} \right| C^N_j \phi^N_j \right\rangle + \sum_{A\neq N}\sum_{B\neq N}\sum_{i\in A}\sum_{j\in B} \left\langle C^A_i \phi^A_i \left| \frac{F^N_{ij}}{r_N^3} \right| C^B_j \phi^B_j \right\rangle \right\} = (A^N_{ij})_1 + (A^N_{ij})_{2,1} + (A^N_{ij})_{2,2} + (A^N_{ij})_3 \qquad (5)$$

where $(A^N_{ij})_1$ and $(A^N_{ij})_3$ are the one- and three-center contributions, respectively. $(A^N_{ij})_{2,1}$ and $(A^N_{ij})_{2,2}$ are two-center contributions, $(A^N_{ij})_{2,2}$ has one atomic orbital centered on nucleus N and $(A^N_{ij})_{2,1}$ has both orbitals centered on the same nucleus, which is not N.

The multicenter integrals were calculated from the MO coefficients by expanding each orbital of the Slater type basis set into five Gaussian type orbitals. Subsequently the integrals were calculated with the program PROPERTY.[32] In Figure 4 the orientations of the calculated and experimental tensors are depicted. The numerical results of the calculations are listed in Table III together with the experimental values and the corresponding data for $Cu(Et_2dtc)_2$.[33] As might be expected on the basis of the LCAO coefficients in Table II, the calculated anisotropic and isotropic HFI for this system is larger than the calculated result for $Cu(Et_2dtc)_2$. This is especially true when this HFI is compared with the extended Hückel result for the latter molecule. The unrestricted Hartree–Fock–Slater method yielded a much larger HFI due to the inclusion of spin-polarization effects. These effects are not expected to be significant for the nitrogen atoms in the present system because there is no nodal plane near these atoms. The multicenter integrals are not dominant but they are significant: ~20% of the largest one-center principal value. The effect of the two- and three-center contribution is a reduction of (the absolute value of) A_1 and A_3, causing the calculated tensors to

Table III. Calculated One-, Two-, and Three-Center Contributions to HFI Tensors of ^{14}N in $Cu(mnt)_2^{2-}$ and $Cu(Et_2dtc)_2$ and the Experimentally Determined Tensors (in MHz)

	one center	two and three center	one, two, and three center	exptl
			dtc-EH[a]	
A_x	−0.03	0.15	0.12	0.18
A_y	0.06	−0.03	0.03	0.18
A_z	−0.03	−0.12	−0.15	−0.36
A_{iso}	0.0	0.0	0.0	−1.124
			dtc-UHFS[b]	
A_x	0.24	0.15	0.39	0.18
A_y	0.48	−0.03	0.45	0.18
A_z	−0.72	−0.12	−0.84	−0.36
A_{iso}	−1.68	0.0	−1.68	−1.124
			mnt N(1)	
A_1	−0.471	0.156	−0.315 (24, x)	−0.318 (34, x)
A_2	−0.477	−0.009	−0.483 (11, z)	−0.486 (25, z)
A_3	0.948	−0.147	0.798 (26, y)	0.804 (24, y)
A_{iso}	0.126	0.051	0.177	0.306
			N(2)	
A_1	−0.420	0.147	−0.273 (21, x)	−0.249 (41, x)
A_2	−0.426	−0.012	−0.435 (9, z)	−0.471 (27, z)
A_3	0.846	−0.135	0.708 (157, y)	0.720 (151, y)
A_{iso}	0.123	0.051	0.174	0.231

[a] One-center interaction calculated from extended Hückel coefficients. [b] One-center interaction calculated from spin densities obtained with an unrestricted Hartree–Fock–Slater calculation.[35]

be nonaxial. This is in agreement with the experiment. The total results for the anisotropic parts are equal to the experimental tensors, both in magnitude and direction, a result that might be fortuitous on the basis of the very crude MO method used. The calculated isotropic HFI is ~50% of the experimental value.

The calculated quadrupole tensors are listed in Table I. Taking into account the approximations in this calculation[34] (only one-center electric field gradient contributions; no lattice contribution) the result is satisfactory: the directions fit the experiment; the principal values are ~50% too large.

Conclusions

In conclusion we can state that the following:

1. The hyperfine and the quadrupole interaction can be measured very accurately, notwithstanding the fact that the spectra are very complicated due to the presence of two nonequivalent nitrogen atoms and the fact that all the interactions are small (i.e. not larger than 2 MHz).
2. The simulation of the ESEEM spectra is remarkably successful, considering the presence of two nitrogen spins. The suppression effect is taken into account by substituting the experimental value of τ in formula 3.
3. The observed splittings of the lines in certain directions of the magnetic field are not understood.
4. The MO calculation gives insight into the electronic structure of the molecule. The agreement between the calculated and the experimental tensors is very satisfactory, especially considering the approximate nature of the MO method.

Acknowledgment. We thank Professor E. de Boer for critically reading the manuscript and stimulating discussions. We are also very grateful to Dr. T. Weeding for correcting the English text.

Registry No. $(n\text{-}Bu_4N)_2(I)$, 15077-49-3; $(NBu_4)_2Ni(mnt)_2$, 18958-57-1.

Contribution from the Istituto di Chimica Generale ed Inorganica, Università di Torino, 10125 Torino, Italy, and Dipartimento di Chimica Inorganica e Metallorganica, Università di Milano, 20133 Milano, Italy

Vibrational Studies of Interstitial Carbide Atoms in Nickel and Rhenium Carbonyl Carbide Clusters

P. L. Stanghellini,*† R. Rossetti,† G. D'Alfonso,‡ and G. Longoni‡

Received May 16, 1986

A vibrational spectroscopy study of the interstitial carbon atom in a series of Re and Ni carbide clusters enabled the M–C vibrational modes to be assigned and the effect of the metal atoms capping the $Re_6(\mu_6\text{-}C)$ and $Ni_8(\mu_8\text{-}C)$ cores to be investigated. The assignment of the M–C vibrational modes has been confirmed by ^{13}C isotopic labeling of the interstitial carbide atom. A single force constant value accounts for the observed frequencies in the nickel carbide clusters, whether capped or uncapped, and in the uncapped rhenium carbide clusters. In contrast, the vibrational analysis for the capped rhenium clusters indicates that the force field around the carbon atom should be described by slightly different axial and equatorial force constants. A rationalization of the capping effect in terms of structural and electronic effects is proposed.

Introduction

Transition-metal carbide clusters have received wide attention in the last decade, probably because of their possible implications with carbon atoms either adsorbed or nested on a metal surface or encapsulated in a metal lattice. As a result, there are now examples of carbide clusters of several transition metals, e.g. Re, Fe, Ru, Os, Co, Rh, and Ni, in which the carbon atom shows a wide spectrum of coordination ranging from μ_4 to μ_8.[1-3]

Since the first complete assignment of the M–C vibrational modes,[4,5] several reports on the vibrational spectra of exposed, semiinterstitial, and interstitial carbide clusters have appeared.[6-12] In the case of interstitial carbide clusters only the octahedral, e.g. $[Fe_6C(CO)_{16}]^{2-}$, $[Ru_6C(CO)_{16}]^{2-}$,[12] and $[Os_{10}C(CO)_{24}]^{2-}$,[7] and trigonal-prismatic, e.g. $Co_6C(CO)_{12}(\mu_3\text{-}S)_2$,[4,5] $[Co_6C(CO)_{15}]^{2-}$, and $[Rh_6C(CO)_{15}]^{2-}$,[10] coordinations of carbon have received

† Università di Torino.
‡ Università di Milano.

(1) Tachikawa, M.; Muetterties, E. L. *Prog. Inorg. Chem.* **1981**, *28*, 301.
(2) Albano, V. G.; Martinengo, S. *Nachr. Chem., Tech. Lab.* **1980**, *28*, 654.
(3) Bradley, J. S. *Adv. Organomet. Chem.* **1983**, *22*, 1.
(4) Bor, G.; Stanghellini, P. L. *J. Chem. Soc., Chem. Commun.* **1979**, 886.
(5) Bor, G.; Dietler, U. K.; Stanghellini, P. L.; Gervasio, G.; Rossetti, R.; Sbrignadello, G.; Battiston, G. A. *J. Organomet. Chem.* **1981**, *213*, 277.
(6) Oxton, I. A.; Powell, D. B.; Farrar, D. M.; Johnson, B. F. G.; Lewis, J.; Nicholls, S. N. *Inorg. Chem.* **1981**, *20*, 4302.
(7) Oxton, I. A.; Kettle, S. F. A.; Jackson, P. F.; Johnson, B. F. G.; Lewis, J. *J. Mol. Struct.* **1981**, *71*, 117.
(8) Oxton, I. A.; Powell, D. B.; Goudsmith, R. J.; Johnson, B. F. G.; Lewis, J.; Nelson, W. J. H.; Nicholls, J. N.; Rosales, M. S.; Vargas, M. D.; Whitmire, K. H. *Inorg. Chim. Acta* **1982**, *64*, L259.
(9) Johnson, B. F. G.; Lewis, J.; Nicholls, J. N.; Owton, I. A.; Raithby, P. R.; Rosales, M. *J. Chem. Soc., Chem. Commun.* **1982**, 289.
(10) Creghton, J. A.; Della Pergola, R.; Heaton, B. T.; Martinengo, S.; Strona, L.; Willis, D. A. *J. Chem. Soc., Chem. Commun.* **1982**, 864.

0020-1669/87/1326-2769$01.50/0